International Journal of Numerical Methods for Heat & Fluid Flow

Two-phase investigation of water-Al_2O_3 nanofluid in a micro concentric annulus under non-uniform heat flux boundary conditions

Davood Toghraie, Ramin Mashayekhi, Hossein Arasteh, Salman Sheykhi, Mohammadreza Niknejadi, Ali J Chamkha,

Two-phase investigation of water-Al_2O_3 nanofluid in a micro concentric annulus under non-uniform heat flux boundary conditions

Received 9 November 2018
Revised 24 November 2018
Accepted 28 November 2018

Davood Toghraie and Ramin Mashayekhi
Department of Mechanical Engineering, Khomeinishahr Branch, Islamic Azad University, Khomeinishahr, Iran

Hossein Arasteh
Department of Mechanical Engineering, Isfahan University of Technology, Isfahan, Iran

Salman Sheykhi and Mohammadreza Niknejadi
Department of Mechanical Engineering, Khomeinishahr Branch, Islamic Azad University, Khomeinishahr, Iran, and

Ali J Chamkha
Department of Mechanical Engineering, Prince Mohammad Bin Fahd University, Al-Khobar, Saudi Arabia

Abstract

Purpose – This is a 3D numerical study of convective heat transfer through a micro concentric annulus governing non-uniform heat flux boundary conditions employing water-Al_2O_3 nanofluid. The nanofluid is modeled using two-phase mixture model, as it has a good agreement to experimental results.

Design/methodology/approach – Half of the inner pipe surface area of the annulus section of a double pipe heat exchanger is exposed to a constant heat flux which two models are considered to divide the exposing surface area to smaller ones considering the fact that in all cases half of the inner pipe surface area has to be exposed to the heat flux: in model (A), the exposing surface area is divided radially to two parts (A1), four parts (A2) and eight parts (A3) by covering the whole length of the annulus and in model (B) the exposing surface area is divided axially to two parts (B1), four parts (B2) and eight parts (B3) by covering half of the annulus radially.

Findings – The results reveal that model (B) leads to higher Nusselt numbers compared to model (A); however, at Reynolds number 10, model (A3) exceeds model (B3). The average Nusselt number is increased up to 142 and 83 per cent at models (A3) with Reynolds number 10 and model (B3) with Reynolds number 1000, respectively.

Originality/value – This paper is a two-phase investigation of water-Al_2O_3 nanofluid in a micro concentric annulus under non-uniform heat flux boundary conditions.

Keywords Two-phase, Nanofluid, Micro annulus non, Non-uniform heat flux

Paper type Research paper

International Journal of Numerical Methods for Heat & Fluid Flow

0961-5539
DOI 10.1108/HFF-11-2018-0628

Nomenclature

A = area [m^2];
C_p = specific heat transfer [J/kg.K];
D = diameter [m];
F = friction coefficient;
F = body force [N];
G = gravitational acceleration [m/s^2];
H = heat transfer coefficient [W/m^2K];
K = thermal conductivity [W/m.K];
Nu = Nusselt number;
Nu = Nusselt number;
Nu_x = local Nusselt number;
L = length [m];
PEC = performance evaluation criteria;
P = pressure [Pa];
q" = heat flux [w/m^2];
Re = Reynolds number;
T = temperature [K];
V = velocity vector [m/s]; and
V = axial velocity [m/s].

Greek Symbols

ϑ = cinematic viscosity [m^2/s];
μ = dynamic viscosity [kg/m.s];
ρ = density [kg/m^3]; and
ϕ = volume fraction of nanoparticles.

Subscripts

ave = average;
b = Bulk;
eff = Effective;
f = Fluid;
i = Inlet;
m = Mixture;
nf = Nanofuid;
o = Outlet;
pl = plain (heat exchanger);
pf = relative viscosity;
w = Wall; and
x = correlated to the *x*-axis.

1. Introduction

Due to the many applications of heat exchangers in various industries, increasing their hydro-thermal performance has been the focus of attention in the thermal design of different engineering systems recently. Consequently, many researchers have investigated various problems around this issue. The proposed approaches for this purpose are the use of nanofluidics and non-uniform boundary conditions including non-uniform heat flux and non-uniform temperature (Ndenguma *et al.*, 2017; Okafor *et al.*, 2018; Wakif *et al.*, 2018).

Because of the low thermal conductivity of conventional heat transfer fluids such as water, oil and so forth, there has been a strong tendency among researchers to develop advanced heat transfer fluid with substantially higher thermal conductivities. To achieve this goal, an innovative and popular way of enhancing the thermal conductivity of conventional fluids is to suspend and stabilize nanoparticles usually with sizes less than 100 nm in fluids named nanofluids. It causes higher thermal conductivities in the conventional fluids to be used in different thermal systems such as different types of heat exchangers (Bhattad *et al.*, 2018; Hosseinnezhad *et al.*, 2018), heat sinks (Kumar and Sarkar, 2018), solar collectors (Subramani *et al.*, 2018) and so forth. Therefore, lots of investigations including numerical, analytical and experimental studies have been performed to achieve a higher thermal performance of such systems using nanofluids in the past two decades.

Lots of efforts have been made to simulate the nanofluids using single-phase and two-phase models. Lee and Mudawar (2007) assessed the thermal effectiveness of Al_2O_3-water nanofluid using single-phase and two-phase models in a microchannel. They showed that using nanofluids causes an improvement in fluid thermal conductivity, cooling effectiveness and thermal boundary layer. Behzadmehr *et al.* (2007) performed a numerical study of turbulent forced convection of Cu-water nanofluid in a tube with uniform heat flux using a two-phase mixture model. They compared the two-phase mixture model and the single-phase model with experimental results which showed that the two-phase mixture model is more precise than the single-phase model. Later, Mirmasoumi and Behzadmehr (2008) performed a similar study and showed that although at the fully developed region, the nanoparticle concentration does not have significant effects on the hydrodynamics parameters, its effects on the thermal parameters are important. Moghari *et al.* (2011) studied the heat transfer enhancement of a mixed convection laminar Al_2O_3-water nanofluid flow in an annulus using two-phase mixture model numerically. They stated that while using nanofluid increases the Nusselt number, its effects on pressure drop is slight as stated by Goodarzi *et al.* (2014) who also concluded this result. Akbari *et al.* (2011) compared CFD predictions of laminar mixed convection of Al_2O_3-water nanofluid using single-phase and three two-phase models including volume of fluid, mixture and Eulerian. They declared that two-phase models predictions are much more close to that of the experiment; however, the predictions by the three two-phase models are essentially the same. Alinia *et al.* (2011) studied the thermal effects of SiO_2-water nanofluid in a cavity using two-phase mixture model and showed that increasing the volume fraction of nanoparticles enhances the thermal performance and changed the flow pattern. Corcione *et al.* (2013) also studied the natural convection in a cavity using the two-phase mixture model to simulate the nanofluid. They introduced an optimal particle loading at which heat transfer performance has a peak. Thereafter, Siavashi *et al.* (2015) investigated a numerical study of convective heat transfer through an annulus using porous media and nanofluid using two-phase mixture model. They introduced an optimum porous media thickness for each nanofluid flowing in a porous medium at a specific Reynolds. Later, other types of nanoparticles were used in thermal-engineering systems using two-phase mixture model which resulted in enhancement in heat transfer (Esfe *et al.*, 2014; Faridzadeh *et al.*, 2014; Keshavarz *et al.*, 2017; Moraveji and Toghraie, 2017; Shareghi and Toghraie, 2016; Toghraie, 2016; Zadkhast *et al.*, 2017). Furthermore, using non-uniform heat flux has been an interesting issue among researchers in boiling studies and distributing the temperature more unit through the geometry (Esfe *et al.*, 2014; Afrand *et al.*, 2016; Sarlak *et al.*, XXXX; Akbari *et al.*, XXXX; Heydari *et al.*, 2017; Pourfattah *et al.*, 2017).

The above literature declares that although many researchers studied various problems including nanofluid modeling by two-phase mixture model and non-uniform heat flux boundary condition, no study has been conducted to investigate the effect of non-uniform boundary condition by dividing that axially and radially through the annulus by using

nanofluid with two-phase mixture model. Therefore, the present study aims to perform such an investigation to reach higher thermal performance in heat exchangers using a new method.

2. Mathematical modeling

This study aims to investigate the influence of heat flux distribution in a concentric annulus using water-Al_2O_3 nanofluid. The present geometry is a double pipe heat exchanger with inner and outer diameters equal to 100 and 200 μm, respectively. Half of the concentric annulus inner wall area is exposed to heat flux equal to 500 kW/m^2, and the outer wall is thermally insulated. The water fluid and three volume concentrations of the nanofluid equal to 1, 2 and 3 per cent enter the annulus section with a uniform temperature of 300 K and velocity with Reynolds numbers equal to 10, 100 and 1000, respectively.

The flow is three-dimensional, laminar, incompressible and steady state. The effects of radiation and natural convection heat transfer are neglected. The water-Al_2O_3 nanofluid is simulated using the two-phase mixture model. A schematic diagram of this study showing the heat flux distributions in two models has been shown in Figure 1.

2.1 Governing equations

The governing equations based on the two-phase mixture model to simulate the nanofluid are defined as follows:

The continuity equation is:

$$\nabla . (\rho_m V_m) = \circ \tag{1}$$

The momentum equation is:

$$\nabla . (\rho_m v_m v_m) = -\nabla p + \nabla . \left[\mu_m \left(\nabla v_m + \nabla v_m^T\right)\right] + \rho_m g + F - \nabla . \left(\sum_{k=1}^{n} \phi_k \rho_k v_{dr,k} v_{dr,k}\right) \tag{2}$$

where F, μ_m, n and $V_{dr,k}$ present the volumetric forces, effective viscosity of the mixture, number of phases and secondary phase of thrust velocity, respectively, which the last parameter is defined as below.

$$V_{dr,k} = V_k - V_m \tag{3}$$

The energy equation is:

$$\nabla \cdot \left[\sum_{k=1}^{n} (\rho_k c_{pk}) \phi_k \vec{V^k} T\right] = \nabla \cdot k_m \nabla T \tag{4}$$

where V_m and ρ_m are mass mean velocity and mixture density, respectively, which are calculated by the following equations.

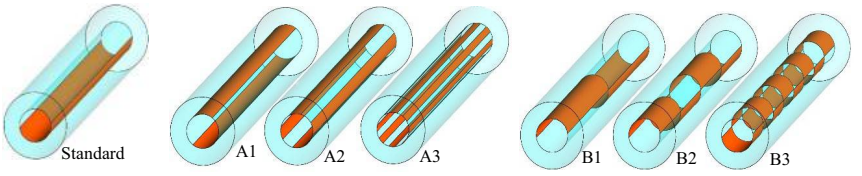

Figure 1.
A schematic diagram of the present study.

$$V_m = \frac{\sum_{1}^{n} \phi_k \rho_k V_k}{\rho_m} \tag{5}$$

$$\rho_m = \sum_{k=1}^{n} \phi_k \rho_k \tag{6}$$

wherein in equation (5), ϕ_k is the volume fraction of the k^{th} phase of the mixture.

The relative velocity for the two-phase is:

$$\vec{V}_{pf} = \vec{V}_p - \vec{V}_f \tag{7}$$

The thrust velocity related to relative velocity is:

$$\vec{V}_{dr,p} = \vec{V}_{pf} - \sum_{k=1}^{n} \frac{\phi_k \rho_k}{\rho_m} \vec{V}_{fk} \tag{8}$$

and mixture viscosity is:

$$\mu_m = \sum_{k=1}^{n} \phi_k \mu_k \tag{9}$$

In this study, the relative velocity presented by Manin (Manninen *et al.*, 1996) and Shiller Newman's drag function (Schiller, 1933) have been used and defined as following equations.

$$\vec{V}_{pf} = \frac{\rho_p d_p^2 (\rho_p - \rho_m)}{18 \mu_f f_{drag} \rho_p} \left(g - \left(\vec{V}_m \cdot \nabla \right) \vec{V}_m \right) \tag{10}$$

$$f_{drag} = \begin{cases} 1 + 0.15 \mathrm{Re}_p^{0.687} \left(\mathrm{Re}_p \leq 1000 \right) \\ 0.0183 \mathrm{Re}_p \left(\mathrm{Re}_p > 1000 \right) \end{cases} \tag{11}$$

Therefore, the thrust velocity as a function of relative velocity is obtained from equation (12).

$$V_{dr,p} = V_{pf} - \sum_{k=1}^{n} \left(\frac{\phi_k \rho_k}{\rho_m} V_{fk} \right) \tag{12}$$

2.2 Nanofluid thermo-physical properties

The water-Al_2O_3 nanofluid density (Khanafer and Vafai, 2011), specific heat capacity (Bianco *et al.*, 2015), effective dynamic viscosity (Maiga *et al.*, 2005) and effective thermal conductivity are defined as the following equations:

$$\rho_{nf} = (1-\phi)\rho_f + \varphi\rho_s \tag{13}$$

$$(\rho C_p) = (1-\phi)(\rho C_p)_f + \phi(\rho C_p)_s \tag{14}$$

$$\mu_{nf} = \frac{\mu_f}{(1-\phi)^{2.5}} \tag{15}$$

$$k_{nf} = 1 + 2.72\phi + 4.97\phi^2 \tag{16}$$

2.3 Boundary conditions

At the inlet of the annulus, uniform temperature and velocity profiles are considered for the water fluid and nanofluid. At its outlet, zero relative pressure is applied. Constant heat flux is used for the sections of the annulus inner wall which is exposed to. Inlet temperature and heat flux are fixed to 300 K and 500 kW/m^2, respectively.

2.4 Data reduction

The local heat transfer coefficient and Nusselt number are:

$$h_x = \frac{q''}{T_w - T_b} \tag{15}$$

$$Nu_x = \frac{h_x D_h}{k_f} \tag{16}$$

The average Nusselt number is:

$$Nu_{ave} = \frac{1}{l}\int_0^l Nu_x dx \tag{17}$$

The friction coefficient calculates by the following equation:

$$f = \left(-\frac{\Delta p}{l}\right)\frac{D_h}{1/2\ \rho v_i^2} \tag{18}$$

and to evaluate the increase in the heat transfer by increasing the pumping power, Performance Evaluation Criteria (PEC) dimensionless number is defined as below. Index "p" corresponds to the plain heat exchanger using water fluid.

$$PEC = \frac{Nu_{ave}/(Nu_{ave})_{pl}}{(f/f_{pl})^{1/3}} \tag{19}$$

3. Numerical simulation

In this study, the three-dimensional simulations with double precision variables have been done using finite volume method. The second-order upwind method has been used to discretize the momentum and energy equations. To couple the velocity and pressure, the SIMPLE scheme has been used. The convergence was considered to have been achieved when the normalized residuals became less than 10^{-6} for all parameters.

3.1 Grid study

To analyze the independence of the solutions from the generated mesh, a structural and non-uniform zonal grid based on the high velocity and temperature gradients on the wall exposed to the heat flux is employed and displayed in Figure 2. To analyze the effect of the grid size on the numerical solution, the average Nusselt number is used to be compared at various grid systems which have been shown in Table I. It is found that after the second case, the relative errors are below 2 per cent; therefore, in view of saving computational time, a grid system with 200,000 cells is chosen for all computations.

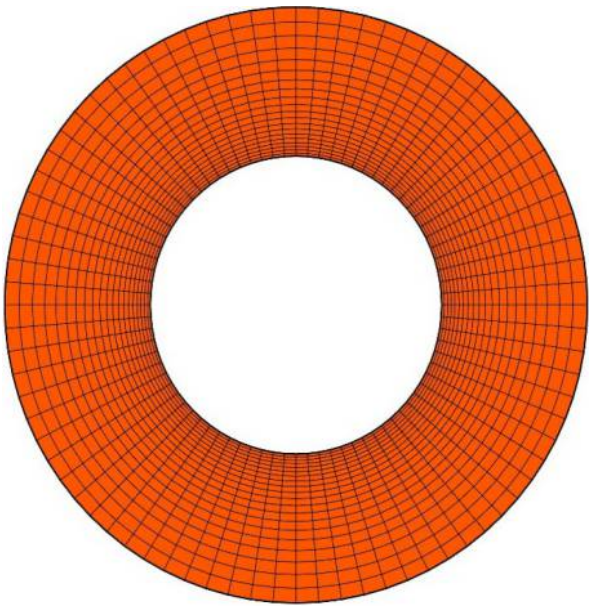

Figure 2.
The generated mesh of the present study

Table I.
Analysis of the solution independency with the grid size

No. of cells	60,000	200,000	500,000	1,000,000	1,500,000
Nu_{ave}	26.1810	28.0488	28.3705	28.2783	28.2701
Error %		6.65	1.13	0.3	0.02

3.2 Validation

To validate the numerical simulation, the experimental study of Wen and Ding (2004) is considered. They investigated the effects of nanofluids on convective heat transfer through a circular straight tube with a constant heat flux condition. The heat transfer coefficient distribution through the pipe is used to compare this simulation and the experimental study. Figure 3 shows a good agreement between this study and with that of Wen and Ding (2004).

4. Results and discussion

At the first stage, half of the inner pipe surface area of the annulus section of the double pipe heat exchanger is exposed to a constant heat flux named "Standard" in Figure 1. Then two models are considered to divide the exposing surface area to smaller ones considering the fact that in all cases half of the inner pipe surface area has to be exposed to the heat flux: in model (A) the exposing surface area is divided radially into two parts (A1), four parts (A2) and eight parts (A3) by covering the whole length of the annulus and in model (B) the exposing surface area is divided axially to two parts (B1), four parts (B2) and eight parts (B3) by covering half of the annulus radially as shown in Figure 1. In the following, the hydro-thermal effects of the mentioned models will be investigated.

Figure 4 represents the local Nusselt number distribution through the length of the annulus for Reynolds number equal to 10 and for the two models with water fluid. It also shows that model (A) improves the local Nusselt number through the annulus in comparison with the standard curve. Dividing the exposing surface area axially enhances the heat diffusion through the annulus cross sections and consequently, the heat flux influences the fluid more effectively. It also causes more uniform temperature distribution in cross-sections through the annulus. It is visible that the local Nusselt number at the thermally fully developed region in models (A1), (A2) and (A3) are equal to about 5.4, 7.5 and 9.5, respectively. As the area between the local Nusselt number and x-axis shows the average Nusselt number, and it is considered as a parameter to evaluate the heat transfer, model (A3) enhances the heat transfer much more than the model (A2), and it is higher than (A1) as well. Figure 3 also displays that model (B) improves the local Nusselt number through the annulus in comparison with the standard curve. Because whenever flow faces new heat flux

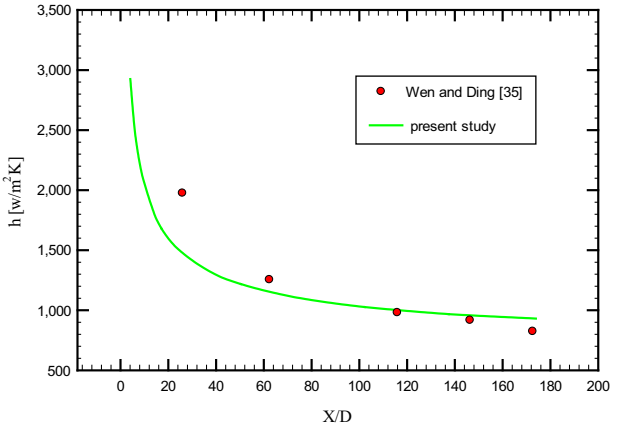

Figure 3.
Comparisons of this study simulation results to experimental data of Wen and Ding (2004)

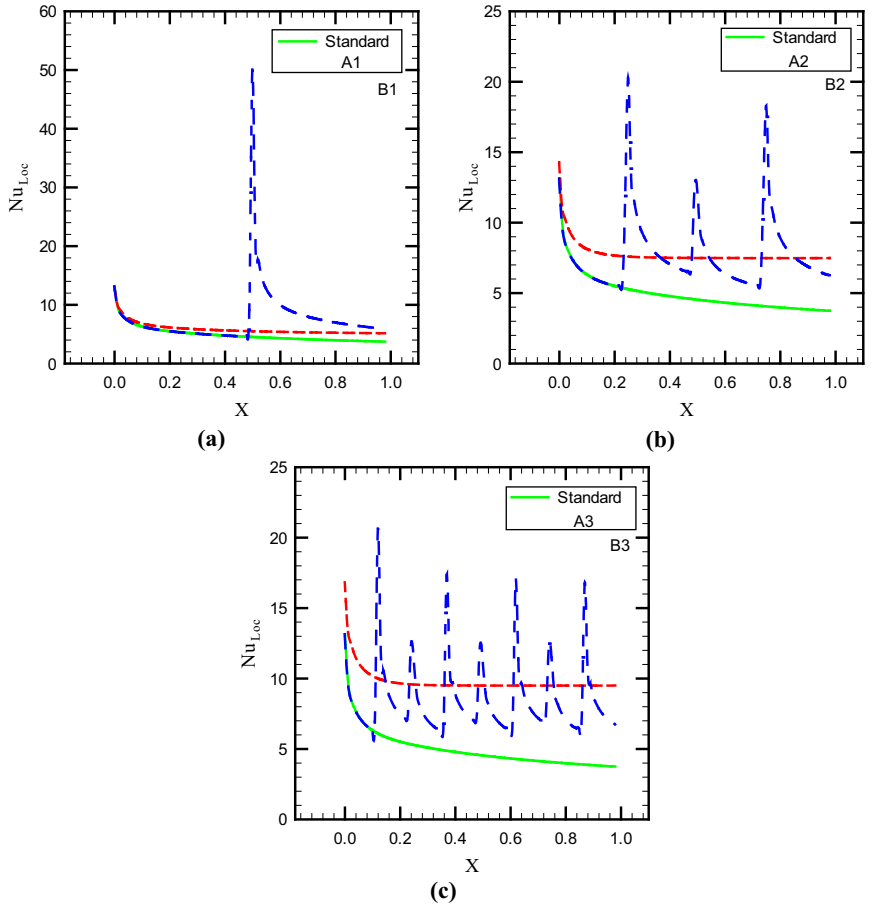

Figure 4.
Local Nusselt number distribution through the length of the annulus for Re = 100 with fluid water

from another side by slicing the exposing surface area axially, the thermal boundary layer is disturbed, and it needs to be generated again with a new thermal entrance region; therefore, it causes a higher amount of heat transfer. Considering the area between the local Nusselt number and *x*-axis, model (B3) enhances the heat transfer much more than the model (B2), and it is higher than (B1) as well. Comparing the two models at each step of division shows that models (B1) and (B2) transfer higher amount of heat than models (A1) and (A2), respectively; on the other hand, model (A3) augments the heat transfer more than model (B3). It is because of the very low thermal entrance region at the model (A3) that the low Reynolds number also affects it, resulting in a Nusselt number at the thermally fully developed region equal to 9.5.

Figures 5 and 6 declare the local Nusselt number distribution through the length of the annulus for Reynolds numbers equal to 100 and 1000, respectively, in the two models with water fluid. This figure shows the effect of Reynolds number on the local Nusselt number and heat transfer. These figures show that increasing the Reynolds number leads to an enhancement in thermal entrance distance which was predictable based on the known

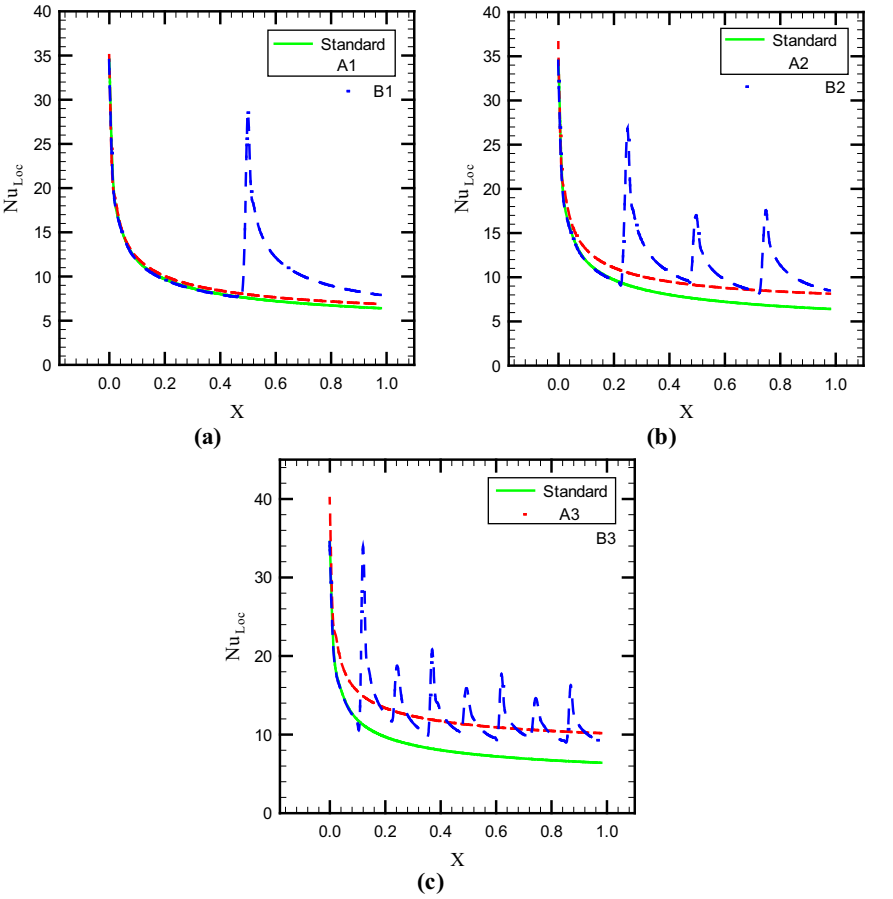

Figure 5.
Local Nusselt number distribution through the length of the annulus for Re = 1000 with fluid water.

formula for thermal entrance distance in laminar flow. Consequently, in model (A), lower differences are visible with the standard curve, and it shows that increasing the Reynolds number reduces the effect of the model (A) on heat transfer augmentation. By contrast, augmenting the Reynolds number increases the effect of the model (B) on heat transfer enhancement. Because in this model, a new thermal boundary layer and a new thermal entrance region are generated with a higher thermal entrance distance. Therefore, the area between the local Nusselt number and *x*-axis increases and as a result the heat transfer enhances.

Figure 7 presents the average Nusselt number for three volume fraction of nanoparticles and three Reynolds numbers to compare the two models at each step of parting the heat flux exposing surface area. It displays that increasing the volume fraction of nanoparticles results in an enhancement in average Nusselt number and heat transfer. It is caused by improving the thermo-physical properties of the fluid by adding the nanoparticles. This figure also shows that model (B) is much more influential on heat transfer and has higher average Nusselt numbers than the model (A)

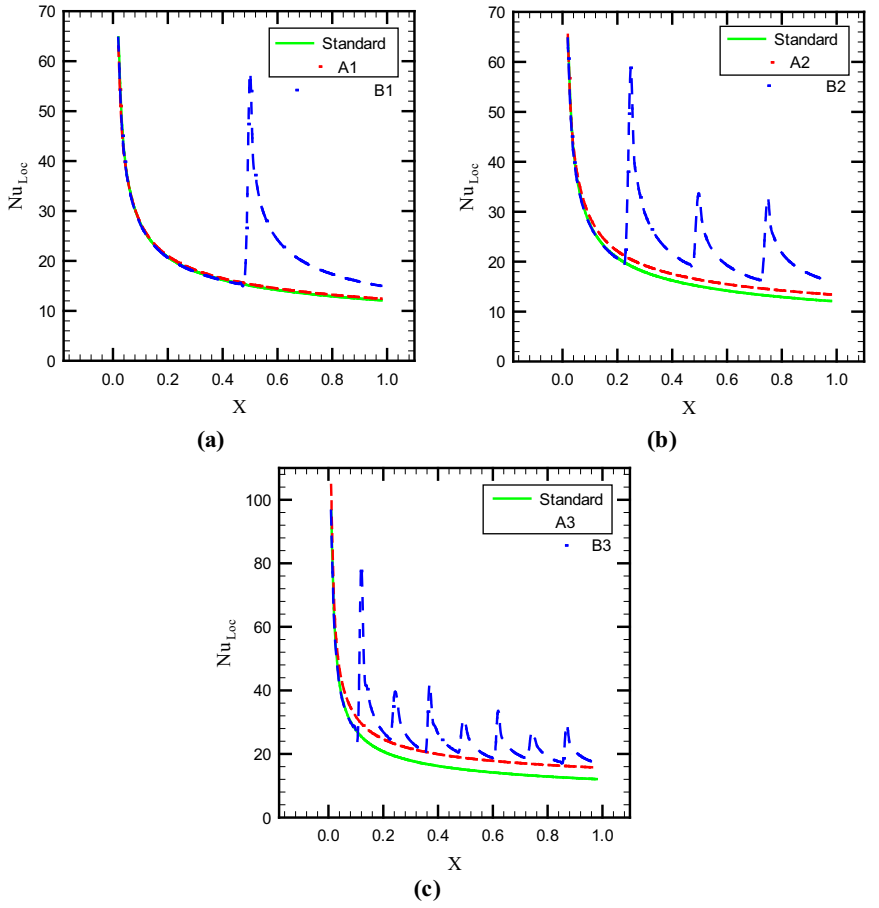

Figure 6.
Variations of the average Nusselt number at each step of parting the heat flux exposing the surface area in the two models for Re = 10, 100, 1000 and ϕ =1%, 2%, 3%.

at Reynolds numbers of 100 and 1000 for three nanoparticle volume concentration which as the number of divisions increases the differences between the curve of two models reduces. It means at higher Reynolds numbers, the effect of disturbing the thermal boundary layer is greater than the effect of heat diffusion through the annulus. But at Reynolds number 10, this trend does not follow. In fact, model (B1) average Nusselt number is higher than the model (A1); models (B2) and (A2) have equal average Nusselt numbers, and model (B3) average Nusselt number is lower than the model (A3). It revealed the fact that at lower Reynolds numbers, the effect of heat diffusion through the annulus is greater than the effect of disturbing the thermal boundary layer.

Figure 8 shows the effect of Reynolds number and nanoparticle volume concentration the on average Nusselt number in the standard case and three steps of division in the model (A). This figure displays that increasing the Reynolds number enhances the Reynolds number in all cases because it augments the velocity gradients on the hot wall and results in an enhancement in heat transfer coefficient near the hot wall. It also shows that the effect of increasing the volume fraction of nanoparticles on the average Nusselt number and heat

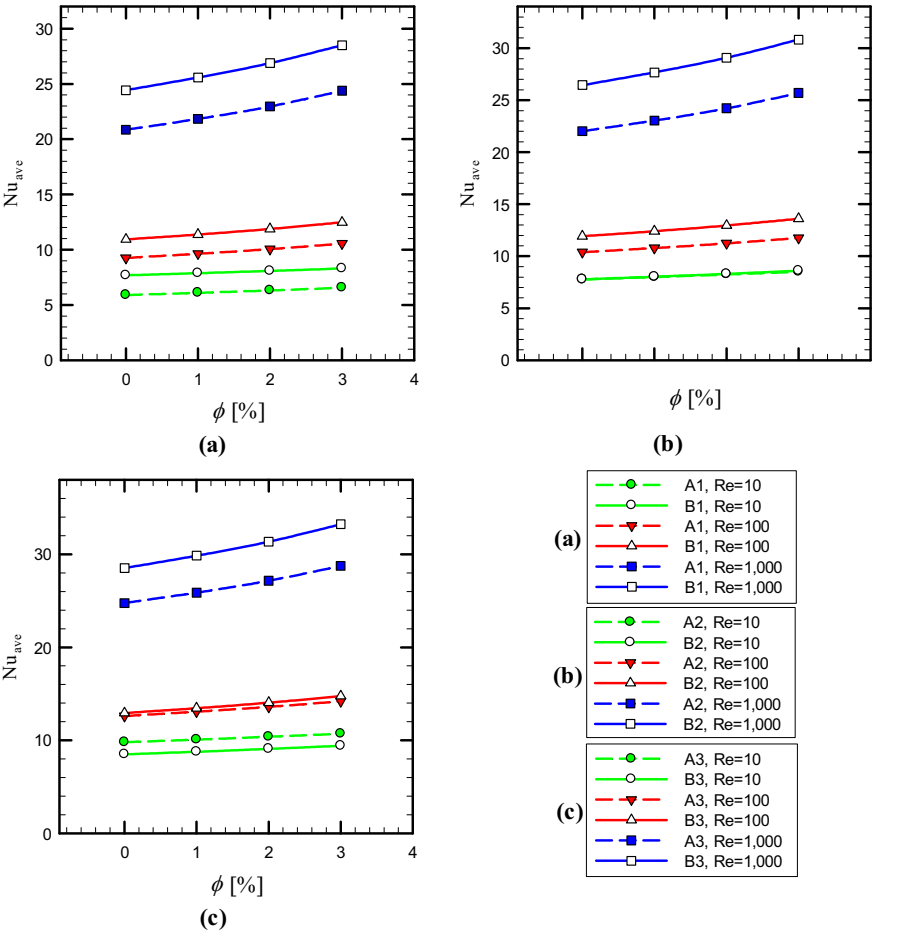

Figure 7.
Variations of the average Nusselt number at each step of parting the heat flux exposing the surface area in the two models for Re = 10, 100, 1000 and $\phi = 1\%, 2\%, 3\%$

transfer as Reynolds number enhances, increases. It is because of higher effects of improvement in thermo-physical properties of the fluid by adding nanoparticles at higher Reynolds numbers. It shows that average Nusselt number for water fluid in the model (A1) is increased up to about 19.1, 4.7 and 3.0 per cent in comparison with the standard case for Reynolds numbers of 10, 100 and 1000, respectively. Also, the average Nusselt number for water fluid in the model (A2) is increased up to about 56.9, 17.4 and 8.8 per cent in comparison with the standard case for Reynolds numbers of 10, 100 and 1000, respectively. Then the average Nusselt number for water fluid in model (A3) is increased up to about 97.7, 42.4 and 22.2 per cent in comparison with the standard case for Reynolds numbers of 10, 100 and 1000, respectively. In the three models in the case with Reynolds number of 10 for the volume fraction of nanoparticles equal to 1, 2 and 3 per cent enhances the average Nusselt number to about 3.4, 7.1 and 11.3 per cent in comparison with the water fluid, respectively. Also for Reynolds number of 100 for the volume fraction of nanoparticles equal to 1, 2 and 3 per cent enhances the average Nusselt number to about 4.0, 8.6 and 14.0 per cent in

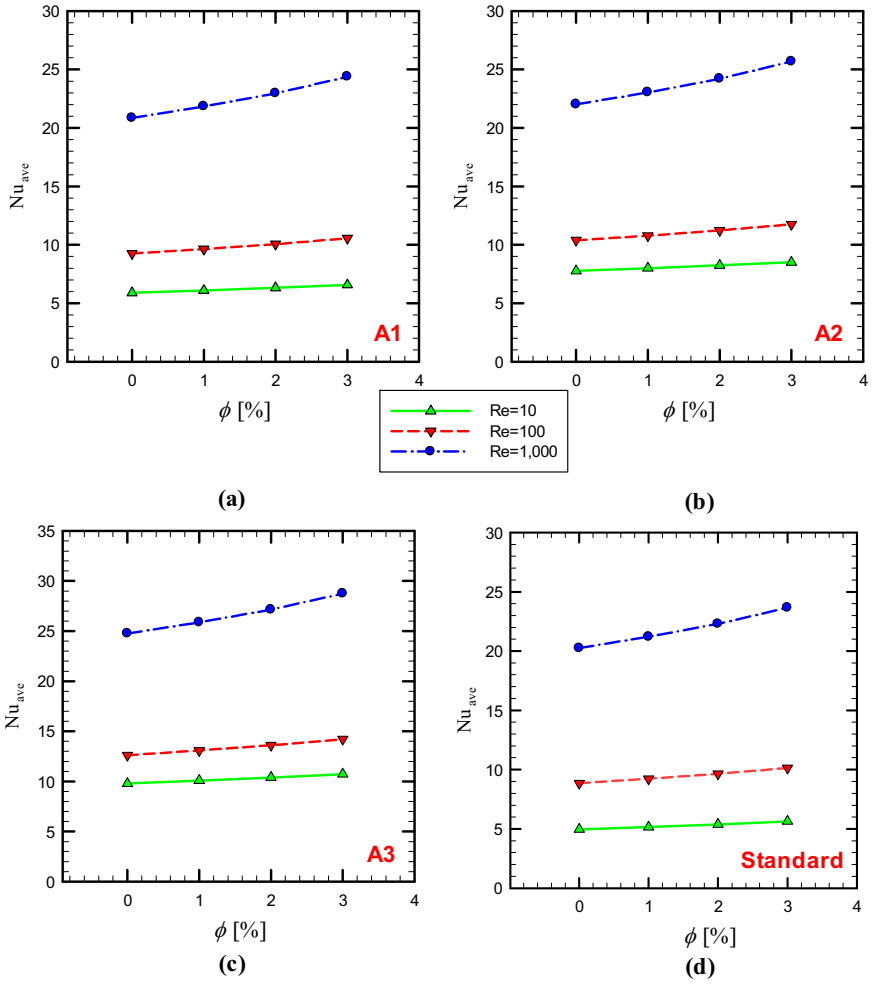

Figure 8.
Variations of the average Nusselt number in the standard case and three steps of division in the model (A) for Re = 10, 100, 1000 and ϕ =1%, 2%, 3%

comparison with the water fluid, respectively. Then for Reynolds number of 1000 for the volume fraction of nanoparticles equal to 1, 2 and 3 per cent enhances the average Nusselt number to about 4.7, and 10.0 and 16.9 per cent in comparison with the water fluid, respectively.

Figure 9 shows the variation of average Nusselt number with the volume fraction of nanoparticles for three Reynolds numbers in the standard case and three steps of division in the model (B). The trend of this figure is so similar to that of Figure 7 but with different values. The causes mentioned in the previous paragraph in the model (A) for enhancing the average Nusselt number by enhancing the Reynolds number and nanoparticles volume concentration is also true for this figure or model (B). It shows that average Nusselt number for water fluid in the model (B1) is enhanced up to about 55.1, 23.4 and 20.7 per cent in comparison with the standard case for Reynolds numbers of 10, 100 and 1000, respectively.

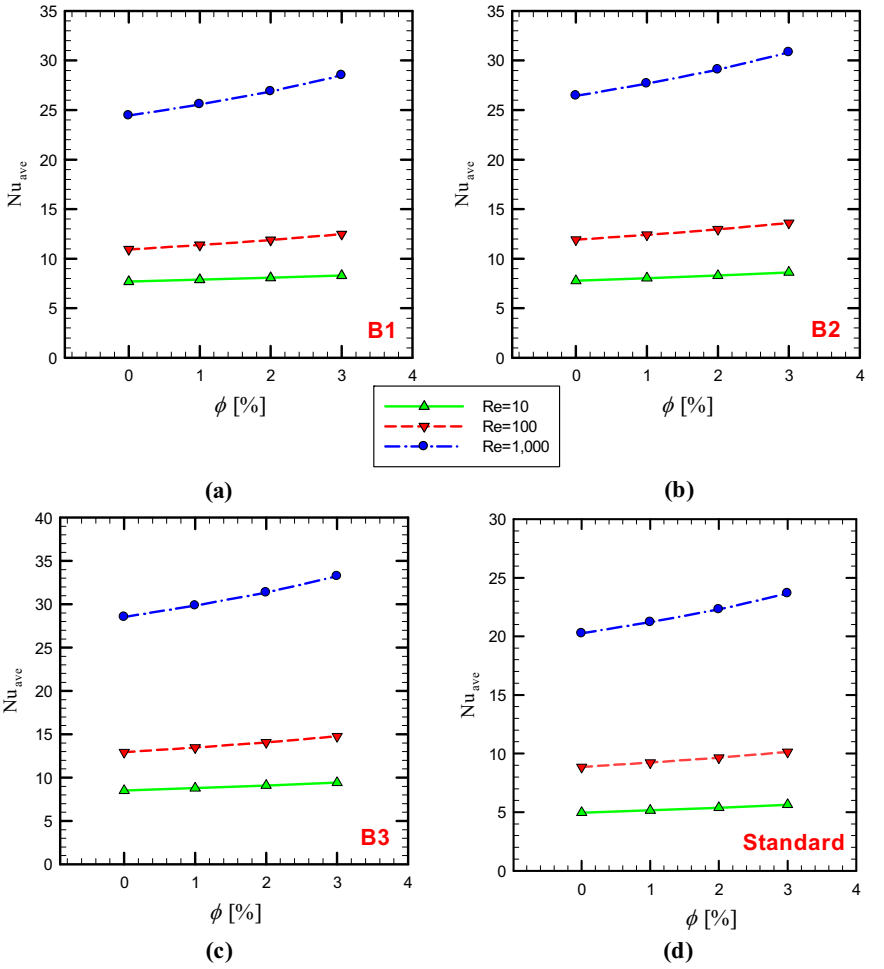

Figure 9.
Variations of the average Nusselt number in the standard case and three steps of division in the model (B) for Re = 10, 100, 1000 and ϕ =1%, 2%, 3%

Also, the average Nusselt number for water fluid in the model (B2) is increased up to about 56.9, 34.6 and 30.6 per cent in comparison with the standard case for Reynolds numbers of 10, 100 and 1000, respectively. Then the average Nusselt number for water fluid in the model (B3) is increased up to about 71.4, 46.0 and 40.8 per cent in comparison with the standard case for Reynolds numbers of 10, 100 and 1000, respectively. In the three models in the case with Reynolds number of 10 for the volume fraction of nanoparticles equal to 1, 2 and 3 per cent enhance the average Nusselt number to about 2.5, 5.1 and 8.0 per cent in comparison with the water fluid, respectively. Also for Reynolds number of 100 for the volume fraction of nanoparticles equal to 1, 2 and 3 per cent enhance the average Nusselt number to about 4.1, 8.7 and 14.2 per cent in comparison with the water fluid, respectively. Then for Reynolds number of 1000 for the volume fraction of nanoparticles equal to 1, 2 and 3 per cent enhance the average Nusselt number to about 4.7, 10.0 and 16.6 per cent in comparison with the water fluid, respectively.

Figure 10 presents the variation of the average friction coefficient with the volume fraction of nanoparticles for three Reynolds numbers. It shows that enhancing the Reynolds number increases the average friction coefficient and it's because of the presence of velocity at its denominator formula (18). It shows that the average friction coefficient at the three Reynolds numbers is increased up to around 3.1, 5.7 and 8.9 per cent in comparison with the water fluid for nanoparticles volume concentration equal to 1, 2 and 3 per cent, respectively.

Figure 11 shows the variation of PEC number with the volume fraction of nanoparticles at both models. It shows the increased heat transfer versus the increased friction coefficient in presence of nanofluid. This figure declares that adding more nanoparticles results in enhancing the PEC number remarkably. It is clearly showing that the highest PEC values correspond to the cases with Reynolds number of 10 which among them the case with nanoparticle volume concentration of 3 per cent, and model (A3) shows the highest PEC value at this model which is equal to 2.16. Model (B) follows a similar trend, and its highest PEC value occurs in the case with Reynolds number of 10, nanoparticle volume concentration of 3 per cent and model (B3) which is equal to 1.90. It is also visible that at both models, increasing the Reynolds number decreases the PEC number. As increasing the Reynolds number and velocity enhances both the heat transfer coefficient and friction coefficient, based on the PEC equation, the increased friction coefficient is higher than the increased Nusselt number and causes lower PEC values.

Ultimately, Figure 12 represents the temperature contours through the annulus for the standard case and both models (A) and (B) at every three steps of their division considering three Reynolds numbers. It shows that in the model (A) dividing the surface area exposed to the heat flux makes the temperature to be distributed through the annulus more uniform and causes higher heat transfer. This figure also displays the effect of the model (B) at each step of division on temperature distribution which shows its effects on this contours that causes better temperature distribution by disturbing the thermal boundary layer as the exposed surface area is divided. Moreover, comparing the contours corresponds to both models with the standard case creates a clearer understanding about the effects of these models on heat transfer.

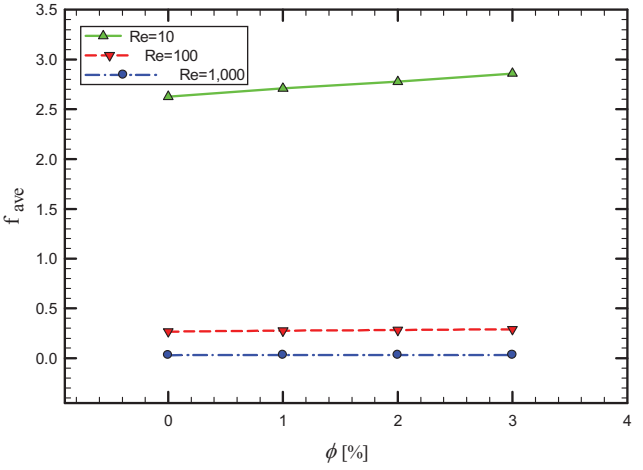

Figure 10. Variation of the average friction coefficient with nanoparticle volume fractions of 1, 2 and 3 per cent for Re= 10, 100, 1000

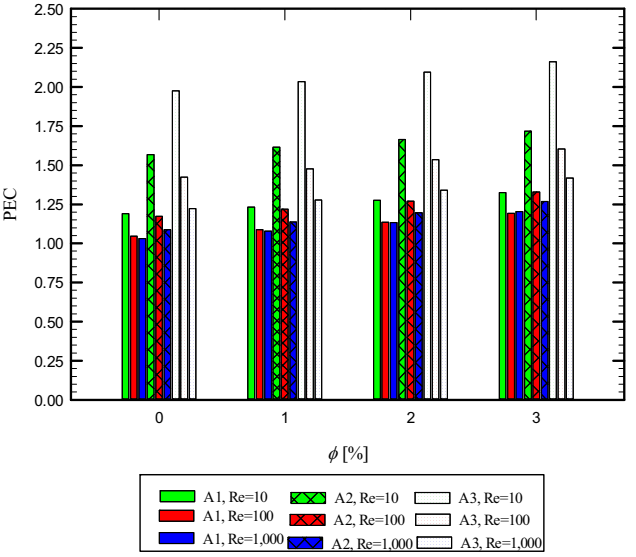

(a)

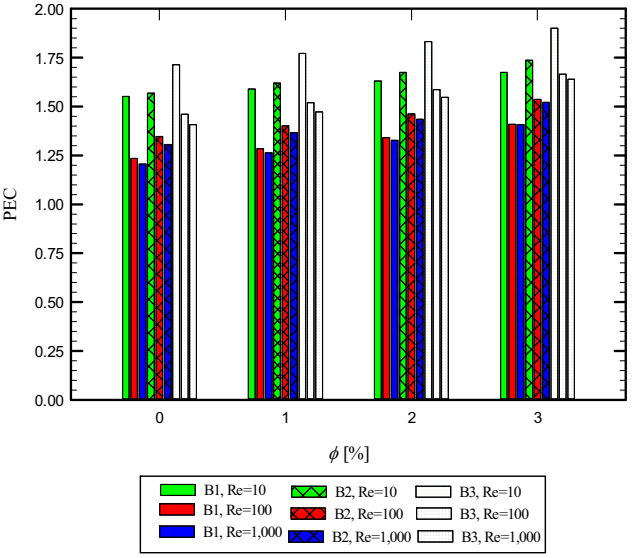

(b)

Figure 11.
Variation of PEC number with nanoparticle volume fractions of 1, 2 and 3 per cent for Re= 10, 100, 1000 at (a) model (A) and (b) model (B)

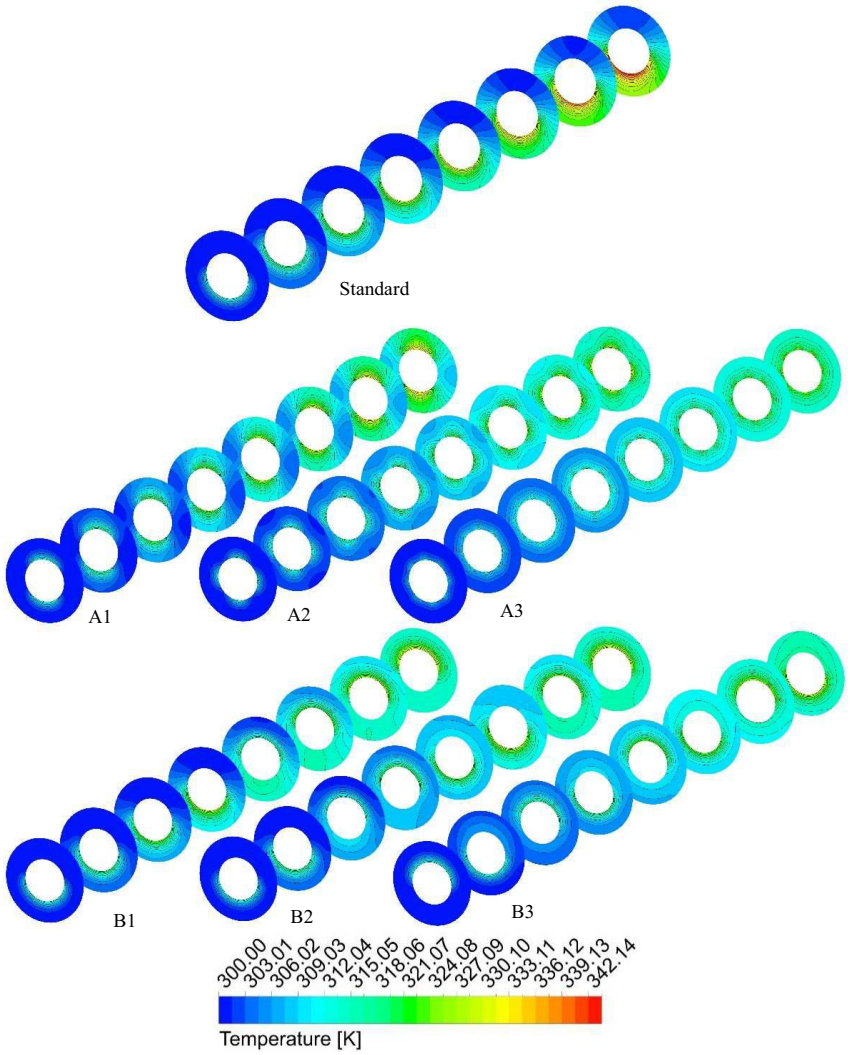

Figure 12.
Temperature contours at standard case and models (A) and (B)

5. Conclusion

This is a three-dimensional numerical investigation of fluid flow and convective heat transfer through a micro concentric annulus with non-uniform heat flux boundary conditions using water-Al_2O_3 nanofluid. The two-phase mixture model is used to simulate the nanofluid and its hydro-thermal effects. Three Reynolds numbers equal to 10,100 and 1000 and three nanoparticle volume concentrations equal to 1, 2 and 3 per cent are analyzed. Half of the inner pipe surface area of the annulus section of a double pipe heat exchanger is exposed to a constant heat flux which two models are considered to divide the exposing surface area to smaller ones considering the fact that in all cases half of the inner pipe surface area has to be exposed to the heat flux: in

model (A), the exposing surface area is divided radially into two parts (A1), four parts (A2) and eight parts (A3) by covering the whole length of the annulus, and in model (B), the exposing surface area is divided axially into two parts (B1), four parts (B2) and eight parts (B3) by covering half of the annulus radially. The obtained results are summarized as follows:

- Dividing the surface area exposed to heat flux through models (A) and (B) results in remarkably higher amount of heat transferring which it is achieved as the model (A) leads to a more uniform distribution of heat flux through the annulus and model (B) causes disturbing the thermal boundary layer.
- The average Nusselt number at the model (B) for three nanoparticle volume fractions is higher than the model (A), except in the cases with Reynolds number of 10 which model (A1) and (B1) are about equivalent, while model (A3) exceeds model (B3) at Reynolds number of 10.
- The average Nusselt number is increased up to 142 and 83 per cent at model (A3) with Reynolds number 10 and model (B3) with Reynolds number 1000, respectively.
- The highest PEC number is obtained at model (A3) with Reynolds number 10 for nanoparticle volume fraction of 3 per cent which is equal to

References

Afrand, M., Toghraie, D. and Ruhani, B. (2016), "Effects of temperature and nanoparticles concentration on rheological behavior of Fe_3O_4 –Ag/EG hybrid nanofluid: an experimental study", *Exp Therm Fluid Sci*, Vol. 77, pp. 2016.

Akbari, M., Galanis, N. and Behzadmehr, A. (2011), "Comparative analysis of single and two-phase models for CFD studies of nanofluid heat transfer", *International Journal of Thermal Sciences*, Vol. 50 No. 8, pp. 1343-1354.

Alinia, M., Ganji, D. and Gorji-Bandpy, M. (2011), "Numerical study of mixed convection in an inclined two sided lid driven cavity filled with nanofluid using two-phase mixture model", *International Communications in Heat and Mass Transfer*, Vol. 38 No. 10, pp. 1428-1435.

Behzadmehr, A., Saffar-Avval, M. and Galanis, N. (2007), "Prediction of turbulent forced convection of a nanofluid in a tube with uniform heat flux using a two phase approach", *International Journal of Heat and Fluid Flow*, Vol. 28 No. 2, pp. 211-219.

Bhattad, A., Sarkar, J. and Ghosh, P. (2018), "Discrete phase numerical model and experimental study of hybrid nanofluid heat transfer and pressure drop in plate heat exchanger", *International Communications in Heat and Mass Transfer*, Vol. 91, pp. 262-273.

Bianco, V., et al., *Heat Transfer Enhancement with Nanofluids*, (2015), CRC press.

Corcione, M., Cianfrini, M. and Quintino, A. (2013), "Two-phase mixture modeling of natural convection of nanofluids with temperature-dependent properties", *International Journal of Thermal Sciences*, Vol. 71, pp. 182-195.

Esfe, M.H., Akbari, M., Semiromi, D.T., Karimiopour, A. and Afrand, M. (2014), "Effect of nanofluid variable properties on mixed convection flow and heat transfer in an inclined two-sided lid-driven cavity with sinusoidal heating on sidewalls", *Heat Transfer Research* , Vol. 45, pp. 409-432.

Esfe, M.H., Saedodin, S., Bahiraei, M., Toghraie, D., Mahian, O. and Wongwises, S. (2014), "Thermal conductivity modeling of MgO/EG nanofluids using experimental data and artificial neural network", *Journal of Thermal Analysis and Calorimetry* , Vol. 118, pp. 287-294.

Faridzadeh, M.R., Semiromi, D.T. and Niroomand, A. (2014), "Analysis of laminar mixed convection in an inclined square lid-driven cavity with a nanofluid by using an artificial neural network", *Heat Transfer Res*, Vol. 45.

Goodarzi, M., et al. (2014), "Investigation of nanofluid mixed convection in a shallow cavity using a two-phase mixture model", *International Journal of Thermal Sciences*, Vol. 75, pp. 204-220.

Heydari, M., Toghraie, D. and Akbari, O.A. (2017), "The effect of semi-attached and offset mid-truncated ribs and water/TiO2 nanofluid on flow and heat transfer properties in a triangular microchannel", *Therm Sci Eng Prog*, Vol. 2, pp. 140-150.

Hosseinnezhad, R., et al. (2018), "Numerical study of turbulent nanofluid heat transfer in a tubular heat exchanger with twin twisted-tape inserts", *Journal of Thermal Analysis and Calorimetry*, Vol. 132 No. 1, pp. 741-759.

Keshavarz, E., Toghraie, D. and Haratian, M. (2017), "Modeling industrial scale reaction furnace using computational fluid dynamics: A case study in Ilam gas treating plant", *Applied Thermal Engineering*, Vol. 123, pp. 277-289.

Khanafer, K. and Vafai, K. (2011), "A critical synthesis of thermophysical characteristics of nanofluids", *International Journal of Heat and Mass Transfer*, Vol. 54 Nos 19/20, pp. 4410-4428.

Kumar, V. and Sarkar, J. (2018), "Two-phase numerical simulation of hybrid nanofluid heat transfer in minichannel heat sink and experimental validation", *International Communications in Heat and Mass Transfer*, Vol. 91, pp. 239-247.

Lee, J. and Mudawar, I. (2007), "Assessment of the effectiveness of nanofluids for single-phase and two-phase heat transfer in micro-channels", *International Journal of Heat and Mass Transfer*, Vol. 50 Nos 3/4, pp. 452-463.

Maiga, S.E.B., et al. (2005), "Heat transfer enhancement by using nanofluids in forced convection flows", *International Journal of Heat and Fluid Flow*, Vol. 26 No. 4, pp. 530-546.,

Manninen, M., Taivassalo, V. and Kallio, S. (1996), *On the Mixture Model for Multiphase Flow*, Technical Research Centre of Finland, Finland.

Mirmasoumi, S. and Behzadmehr, A. (2008), "Numerical study of laminar mixed convection of a nanofluid in a horizontal tube using two-phase mixture model", *Applied Thermal Engineering*, Vol. 28 No. 7, pp. 717-727.

Moghari, R.M., et al. (2011), "Two phase mixed convection Al_2O_3 – water nanofluid flow in an annulus", *International Journal of Multiphase Flow*, Vol. 37 No. 6, pp. 585-595.,

Moraveji, A. and Toghraie, D. (2017), "Computational fluid dynamics simulation of heat transfer and fluid flow characteristics in a vortex tube by considering the various parameters", *International Journal of Heat and Mass Transfer*, Vol. 113, pp. 432-443.

Ndenguma, D.D., Dirker, J. and Meyer, J.P. (2017), "Transitional flow regime heat transfer and pressure drop in an annulus with non-uniform wall temperatures", *International Journal of Heat and Mass Transfer*, Vol. 108, pp. 2239-2252.

Okafor, I.F., Dirker, J. and Meyer, J.P. (2018), "Asymmetrical Non-Uniform heat flux distributions for laminar flow heat transfer with mixed convection in a horizontal circular tube", *Heat Transfer Engineering*, pp. 1-19.

Pourfattah, F., Motamedian, M., Sheikhzadeh G., Toghraie, D. and Akbari, O.A. (2017), "The numerical investigation of angle of attack of inclined rectangular rib on the turbulent heat transfer of Water-Al2O3 nano-fluid in a tube", *Int J Mech Sci*, Vols 131–132, pp. 1106-1116.

Schiller, L. (1933), "A drag coefficient correlation", *Zeit. Ver. Deutsch. Ing*, Vol. 77, pp. 318-320.

Shareghi, S. and Toghraie, D. (2016), "Numerical simulation of blood flow in healthy arteries by use of the sisko model", *Computational Thermal Sciences: An International Journal* , Vol. 8 No. 4, pp. 309-320.

Siavashi, M., Bahrami, H.R.T. and Saffari, H. (2015), "Numerical investigation of flow characteristics, heat transfer and entropy generation of nanofluid flow inside an annular pipe partially or completely filled with porous media using two-phase mixture model", *Energy*, Vol. 93, pp. 2451-2466.

Subramani, J., et al. (2018), "Efficiency and heat transfer improvements in a parabolic trough solar collector using TiO 2 nanofluids under turbulent flow regime", *Renewable Energy*, Vol. 119, pp. 19-31.,

Toghraie, D. (2016), "Numerical thermal analysis of water's boiling heat transfer based on a turbulent jet impingement on heated surface", *Physica E*, Vol. 84, pp. 454-465.

Wakif, A., et al. (2018), "Numerical analysis of the unsteady natural convection MHD couette nanofluid flow in the presence of thermal radiation using single and Two-Phase nanofluid models for Cu–Water nanofluids", *International Journal of Applied and Computational Mathematics*, Vol. 4 No. 3, pp. 81.,

Wen, D. and Ding, Y. (2004), "Experimental investigation into convective heat transfer of nanofluids at the entrance region under laminar flow conditions", *International Journal of Heat and Mass Transfer*, Vol. 47 No. 24, pp. 5181-5188.

Zadkhast, M., Toghraie, D. and Karimipour, A. (2017), "Developing a new correlation to estimate the thermal conductivity of MWCNT-CuO/Water hybrid nanofluid via an experimental investigation", *Journal of Thermal Analysis and Calorimetry* , Vol. 129 No. 2, pp. 859-867.

Further reading

Akbari, O.A. Afrouzi, H.H. Marzban, A. Toghraie, D. Malekzade, H. and Arabpour, A. "Investigation of volume fraction of nanoparticles effect and aspect ratio of the twisted tape in the tube", *J Therm Anal Calorim*, doi: 10.1007/s10973-017-6372-7

Sarlak, R. Yousefzadeh, S. Akbari, O.A. Toghraie, D. Sarlak, S. and assadi, F. (2017), "The investigation of simultaneous heat transfer of water/Al2O3 nanoßuid in a close enclosure by applying homogeneous magnetic field", *International Journal of Mechanical Sciences*, Vol. 133, pp. 674-688, doi: 10.1016/j.ijmecsci.2017.09.035.

Corresponding author

Davood Toghraie can be contacted at: davoodtoghraie@gmail.com